$$|\beta_{dp}(\mathbf{k})|^2 = 2\beta_{dp}{}^2[2 - \cos(k_x a) - \cos(k_y a)] \quad \text{(A4)}$$

The solution to the secular equation is:

$$\epsilon(\mathbf{k}) = \langle\epsilon_{dp}\rangle \pm \sqrt{(\Delta\epsilon_{dp}/2)^2 + |\beta_{dp}(\mathbf{k})|^2} \quad \text{(A5)}$$

where $\langle\epsilon_{dp}\rangle = (\epsilon_d + \epsilon_p)/2$ and $\Delta\epsilon_{dp} = |\epsilon_d - \epsilon_p|$. Eliminating $\langle\epsilon_{dp}\rangle$ by choice of the energy zero, an exact solution for the density of states, $g(\epsilon)$, can be obtained from the formula for the band dispersion in eq A5:

$$g(\epsilon) = \frac{4|\epsilon|}{\pi^2\beta_{dp}{}^2}K([E^2(2 - E^2)]^{1/2}] \quad \text{(A6a)}$$

$K(z)$ is a complete elliptic integral of the first kind;[21] E is restricted to the range $0 \le E^2 \le 2$ and is related to ϵ by the equation:

$$E^2 = \frac{\epsilon^2 - (\Delta\epsilon_{dp}/2)^2}{4\beta_{dp}{}^2} \quad \text{(A6b)}$$

The π DOS has the form shown in Figure 2 where $\Delta\epsilon_{dp} = 1.0$ eV, and $|\beta_{dp}| = 1.8$ eV.

The form of the Wannier functions for the superdegenerate band can be determined from eq 10 and A1:

$$\omega(0) = \frac{1}{N^{1/2}}\sum_{\mathbf{k}}^{BZ}\chi(\mathbf{k}) = N^{1/2}(a/2\pi)^2\int_{-\pi/a}^{\pi/a}\int\chi(\mathbf{k})\,dk_x\,dk_y \quad \text{(A7)}$$

where the Wannier function considered is that centered on the origin ($\mathbf{R} = 0$). After simplification, expressions for the Wannier function coefficients can be derived. The magnitude of the "inner" orbital coefficients illustrated in **15b** was determined by numerical integration:

$$\frac{4}{\pi^2}\int_{2^{-1/2}}^{1}\frac{E(x) - x_1{}^2K(x)}{x_1x^2\sqrt{2x^2 - 1}}\,dx \approx 0.47239 \quad \text{(A8)}$$

$K(x)$ and $E(x)$ are complete elliptic integrals of the first and second kind, respectively, and $x_1 \equiv (1 - x^2)^{1/2}$. This value indicates that 89.3% of the electron density resides on the "inner" centers, which is to be compared to 100% implied by **15a**. The remainder of the electron density resides on centers further removed.

Appendix II

All the computations were carried out using a program employing the extended Hückel method[22a] which may be used for both molecular and crystal calculations. It has been developed to its present state by M.-H. Whangbo, S. Wijeyesekera, M. Kertesz, C. N. Wilker, C. Zheng, and the author. The weighted Wolfsberg–Helmholz formula[22b,c] was used for the H_{ij} matrix elements. Pt and As parameters were taken from ref 6; Mo parameters are from ref 23. Exponents for P and As are originally from ref 24; the P p orbital energy was extrapolated from Herman–Skillman[25] tables so that is in alignment with EH parameters of adjacent elements of the periodic table. Exponents for the transition metals are originally from ref 26. See Table I.

In the results reported for $^2_\infty[Pt_3(As_2)_2{}^{2-}]$ and $^2_\infty[MoH_2P]$ layers in Figures 4 and 5, matrix elements were computed between atoms separated by less than 6.55 Å. Both are two dimensional hexagonal systems in which $^1/_{12}$th of the Brillouin zone was covered by **k**-point meshes: 105 points were used for $^2_\infty[Pt_3(As_2)_2{}^{2-}]$; 300 points were used for $^2_\infty[MoH_2P]$.

(21) (a) Whittaker, E. T.; Watson, G. N. "Modern Analysis", 4th ed.; Cambridge University Press: Cambridge, 1927. (b) Gradshteyn, I. S.; Ryzhik, I. M. "Tables of Integrals, Series, and Products", 4th ed.; Academic Press: New York, 1965.

(22) (a) Hoffmann, R. *J. Chem. Phys.* **1963**, *39*, 1397. (b) Ammeter, J. H.; Bürgi, H.-B.; Thibeault, J. C.; Hoffmann, R. *J. Am. Chem. Soc.* **1978**, *100*, 3686. (c) Summerville, R. H.; Hoffmann, R. *Ibid.* **1976**, *98*, 7240.
(23) Kubácek, P.; Hoffmann, R.; Havlas, Z. *Organometallics* **1982**, *1*, 180.
(24) Clementi, E.; Roetti, C. *At. Nucl. Data Tables* **1974**, *14*, 177.
(25) Herman, F.; Skillman, S. "Atomic Structure Calculations"; Prentice Hall: Englewood Cliffs, N.J., 1963.
(26) Baranovskii, V. I.; Nikolskii, A. B. *Teor. Eksp. Khim.* **1967**, *3*, 527.

Gas-Phase Isotope Fractionation Factor for Proton-Bound Dimers of Methoxide Anions

David A. Weil[†] and David A. Dixon*[‡]

Contribution from the Department of Chemistry, University of California—Riverside, Riverside, California 92521, and E. I. du Pont de Nemours & Co., Central Research and Development Department, Experimental Station, Wilmington, Delaware 19898. *Received June 8, 1984*

Abstract: The gas-phase isotope fractionation factor, ϕ_{gp}, for A_2L^- (where A = MeO and L = H or D) has been measured by ion cyclotron resonance spectroscopy. The value for ϕ_{gp} is 0.33 ± 0.06. The gas-phase value is compared with the solution measurements. Ab initio calculations on the electronic structure of the dimer have been performed at the DZ+P level. The dimer is found to be asymmetric with a central barrier to proton transfer on the order of 2 kcal/mol. The harmonic force field for the dimer has been determined with the 4-31G basis set. These results are used to calculate a theoretical value for ϕ_{gp} of 0.37 in excellent agreement with the experimental value. The calculated hydrogen bond strength is 25.6 kcal/mol.

Over the past 15 years, determinations of proton transfer equilibrium constants have increased the understanding of gas-phase reaction dynamics and the effect that solvent molecules have on analogous solution-phase equilibrium.[1] In contrast, the rates of proton transfer reactions are not as easily determined in either the gas or solution phase, especially when the proton donor–acceptor separation is small.[2] A description of the potential energy surface for small proton–acceptor separation would aid in the

[†] University of California—Riverside.
[‡] E. I. du Pont de Nemours & Co. Contribution No. 3755.

(1) (a) D. H. Aue and M. T. Bowers In "Gas Phase Ion Chemistry", M. T. Bowers, Ed., Academic Press, New York, 1979, Vol. 2, C9. (b) R. W. Taft In "Proton-Transfer Reactions", E. Caldin and V. Gold, Eds., Wiley, New York, 1975, p 31. (c) E. M. Arnett, Ibid., p 79. (d) E. M. Arnett, *Acc. Chem. Res.*, **6**, 404 (1973). (e) R. W. Taft In "Progress in Physical Organic Chemistry", R. W. Taft, Ed., Vol. 14, p 247, 1983, Wiley-Interscience, New York.

0002-7863/85/1507-6859$01.50/0

separation of intrinsic and solvation effects on the rates of proton transfer reactions.

The use of the isotopes of hydrogen has proven to be a very sensitive technique for studying proton transfer reactions in solution.[3] Similar use of isotopes in the gas phase has only recently been initiated.[4] Because gas-phase proton transfers generally occur at or near the ion–molecule collision rate ($k = 1\text{–}2 \times 10^9$ cm^3 molecules^{-1} s^{-1}), kinetic isotope effects (KIE) are usually difficult to observe.[5] Equilibrium isotope effects (EIE) can be observed by using the technique of ion cyclotron resonance (ICR) spectroscopy,[6] and such effects can then be used to obtain information about the potential describing the motion of the proton. This should lead to further insight on the effects of solvent on the proton transfer.

Our approach to the study of intramolecular proton transfers and solvent effects is to determine gas-phase proton transfer equilibrium constants for isotopically substituted species in an ion cyclotron resonance spectrometer. Specifically we determine the isotope fractionation factor for the bridging proton in proton-bound dimer anions. Kreevoy and co-workers[7,8] have recently determined the isotope fractionation factors in the solution phase for a number of homoconjugate complexes A_2L^-, where L is a positively charged isotope of hydrogen (the lyate ion) and A^- is some anion, e.g., 4-nitrophenolate. The isotope fractionation factor ϕ can be defined as the ratio $(\chi_D/\chi_H)_{solute}/(\chi_D/\chi_H)_{solvent}$ for the chemically exchangeable protons where χ is the appropriate activity. For example, for an acid LA with a single exchangeable hydrogen, ϕ becomes equal to

$$\phi = \{[DA]/[HA]\}/\{x/(1-x)\}$$

where x is the fraction of deuterated solvent present. In solution, isotope fractionation factors are usually measured in a nonexchanging solvent with two exchangeable solutes. One solute is then related back to a standard state of a 50:50 mixture of liquid HOD and H_2O. In the experiments discussed below, the gas-phase isotope fractionation factors are obtained from the measurement of equilibrium constants for ligand exchange reactions of the form of reaction 1. The equilibrium constant K_1 for reaction 1 is equal

$$[A\text{--}H\text{--}A]^- + DA \rightleftharpoons [A\text{--}D\text{--}A]^- + HA \qquad (1)$$

to the ratio of the gas-phase isotope fractionation factor of the proton-bound dimer of A^-, $\phi(ALA^-)$, and that for AL, $\phi(AL)$, both of which are related back to the standard state, in this case H_2O.

$$K_1 = ([ADA]^-/[AHA]^-)([AH]/[AD]) \qquad (2a)$$

$$= \phi(ALA)^-/\phi(AL) \qquad (2b)$$

The gas-phase isotope fractionation factor for the proton-bound dimer of the ethoxide anion has previously been measured, $\phi_{gp}(A = EtO^-) = 0.46 \pm 0.1$, using the proton transfer equilibrium given below in (3).[9] We have now determined the gas-phase isotope

$$[EtOHOEt]^- + EtOD \rightleftharpoons [EtODOEt]^- + EtOH \qquad (3)$$

$$K_3 = \phi(EtOLOEt^-)/\phi(EtOL)$$

fractionation factor for the proton-bound dimer of methoxide anion. An important reason for measuring $\phi(A = OMe^-)$ is that, unlike the case for $A = OEt^-$, the isotope fractionation factor for $A = OMe^-$ has been recently determined in the solution phase.[10] Furthermore, the decrease in the number of degrees of freedom makes the system more tractable for theoretical study. By comparing the gas-phase and solution-phase work, the effect of solvation on the value for ϕ can be observed, and from a comparison of the values of ϕ for $A = OEt^-$ and OMe^-, the effect of alkyl group size can be postulated.

Kreevoy et al.[7,8] have suggested that the isotope fractionation factors can be used to predict the qualitative shape of the potential energy surface for small proton donor–acceptor separation. The qualitative features of the surface predicted from the isotope fractionation factor can be compared with portions of the surface calculated from ab initio molecular orbital theory. There are some ab initio calculations[11,12] available for the $[MeO\text{–}H\text{–}OMe]^-$ surface at the SCF level using 4-31G basis sets. The geometry of this complex suggests that the proton is not bonded in the center of the potential but rather is preferentially bonded to one MeO^- group giving a double-well potential. Even more accurate calculations including correlation corrections are available for the $[HO\text{–}H\text{–}OH]^-$ surface,[13,14] and although a double-well potential is found, the barrier to proton transfer is predicted to be very low, 0.15 kcal/mol at the SCF–CI level.[13] In order to better understand the potential energy surface for $[MeO\text{–}H\text{–}OMe]^-$, extensive ab initio calculations have been performed, including a vibrational analysis of the dimer.

Experimental and Computational Details

Experiments were carried out with use of ion cyclotron resonance (ICR) spectrometry.[15,16] The ICR was a modified Varian 5900 spec-

Scheme I

$$MeONO \xrightarrow{e^-} MeO^- + NO \qquad (4)$$

$$MeO^- + MeOCHO \longrightarrow [MeOHOMe]^- + CO \qquad (5)$$

$$[MeOHOMe]^- + MeOD \rightleftharpoons [MeODOMe]^- + MeOH \qquad (6)$$

1a (m/e=63) **1b** (m/e=64)

(2) W. E. Farneth and J. I. Brauman, *J. Am. Chem. Soc.*, **98**, 7891 (1976). General models for proton transfer between a neutral and an anion usually include an initial complex formed between the neutral proton donor and the anion which is separated by a barrier from the regime where proton transfer actually occurs. It is this latter regime which we define as that where the proton donor–acceptor separation is small. The experimental measurement of the rate constant is for the overall transfer process and it is difficult to determine if the rate constant measures the formation of the initial complex, the actual proton transfer step, or some combination of the two.

(3) (a) R. P. Bell In "The Proton in Chemistry", 2nd ed., Cornell University Press, Ithaca, 1973. (b) F. H. Westheimer, *Chem. Rev.*, **61**, 265 (1961). (c) R. P. Bell, *Chem. Soc. Rev.*, **3**, 513 (1974). (d) R. A. More-O'Ferrall, "Proton-Transfer Reactions", E. Caldin and V. Gold, Eds., Wiley, New York, p 201, 1975. (e) L. B. Sims, A. Fry, D. E. Lewis, and L. T. Netherton In "Synthesis and Applications of Isotopically Labeled Compounds", Eds. W. P. Duncan and A. B. Susanm, Eds., Elsevier Scientific Publishing Co., Amsterdam, p 261, 1983. (f) M. M. Kreevoy In "Isotopes in Organic Chemistry", E. Buncel and C. C. Lee, Eds., Elsevier Scientific, New York, 1975.

(4) (a) J. M. Jasinski and J. I. Brauman, *J. Am. Chem. Soc.*, **102**, 2906 (1980). (b) M. T. Bowers; D. D. Elleman, and J. L. Beauchamp, *J. Phys. Chem.*, **72**, 3599 (1968). (c) S. E. Buttrill, *J. Chem. Phys.*, **52**, 6174 (1970). (d) J. L. Beauchamp and M. C. Caserio, *J. Am. Chem. Soc.*, **94**, 2638 (1972). (e) J. C. Wilson and J. H. Bowie, *Aust. J. Chem.*, **28**, 1993 (1975). (f) J. A. Benbow, J. C. Wilson, and J. H. Bowie, *Int. J. Mass Spectrom. Ion Phys.*, **26**, 1973 (1978). (g) K. M. Weillman, W. E. Victoriano, P. C. Isolani, and J. M. Riveros, *J. Am. Chem. Soc.*, **101**, 2242 (1979).

(5) (a) D. K. Bohme, "Interactions Between Ions and Molecules", P. Ausloss, Ed., Plenum Press, New York, p 489, 1975. (b) R. S. Hemsworth, J. D. Payzant, H. I. Schiff, and D. K. Bohme, *Chem. Phys. Lett.*, **26**, 417 (1974). (c) D. Betowski, J. D. Payzant, G. I. Mackay, and D. K. Bohme, *Chem. Phys. Lett.*, **31**, 321 (1975). (d) G. I. Mackay, L. D. Betowski, J. D. Payzant, H. I. Schiff, and D. K. Bohme, *J. Phys. Chem.*, **80**, 2919 1976. (e) C. G. Freeman, P. W. Freeman, P. W. Harland, and M. J. McEwan, *Aust. J. Chem.*, **31**, 2157 (1978).

(6) (a) J. F. Wolf, J. L. Devlin, III, and R. W. Taft, *J. Am. Chem. Soc.*, **98**, 287 (1976). (b) J. F. Wolf, J. L. Devlin, III, D. J. DeFrees, R. W. Taft, and W. J. Hehre, *J. Am. Chem. Soc.*, **98**, 5097 (1976). (c) D. E. Sunko, I. Szele, and W. J. Hehre, *J. Am. Chem. Soc.*, **99**, 5000 (1977).

(7) M. M. Kreevoy, T. M. Liang, and K. C. Chang, *J. Am. Chem. Soc.*, **102**, 3315 (1980).

(8) M. M. Kreevoy, T. M. Liang, and K. C. Chang, *J. Am. Chem. Soc.*, **99**, 5207 (1977).

(9) M. R. Ellenberger, W. E. Farneth, and D. A. Dixon, *J. Phys. Chem.*, **85**, 4 (1981).

(10) (a) L. Baltzer, Ph.D. Thesis, University of Gothenburg, 1981. (b) V. Gold and S. Grist, *J. Chem. Soc. B*, 1665 (1971).

(11) W. Jorgenson and M. Ibrahim, *J. Comput. Chem.*, **2**, 7 (1981).

(12) G. Klass, J. C. Sheldon, and J. C. Bowie, *Aust. J. Chem.*, **35**, 2471 (1982).

(13) B. O. Roos, W. P. Kraemer, and G. H. F. Diercksen, *Theor. Chim. Acta*, **42**, 77 (1976).

(14) S. Schneiner, M. M. Szczesniak, and L. D. Bigham, *Int. J. Quantum Chem.*, **23**, 739 (1983).

(15) J. L. Beauchamp, *Annu. Rev. Phys. Chem.*, **22**, 527 (1971).

(16) J. E. Bartmess and R. T. McIver, Jr., In "Gas Phase Ion Chemistry", M. T. Bowers, Ed., Academic Press, Vol. 2, p 89, 1979, and references therein.

Table I. Summary of Pressure Ratio Effects on K_6

P_1/P_2[a]	10^5P_{TOT}[b]	no. of exptl points[c]	I_{63}[d]	I_{64}	I_{64}/I_{63}	MeOH/MeOD[e]	K_6[f]
0.67	2.5	6	0.648	0.352	0.543	0.227	0.123
1.4	3.6	4	0.551	0.450	0.816		0.185
2.2	4.8	8	0.494	0.506	1.025		0.233
3.0	6.0	6	0.460	0.540	1.172		0.266*
3.9	7.3	5	0.462	0.538	1.165		0.264*
0.23	3.2	2	0.656	0.344	0.525	0.200	0.105
0.38	3.6	2	0.622	0.378	0.608		0.122
0.62	4.2	2	0.586	0.414	0.707		0.141
0.78	3.2	2	0.582	0.419	0.720		0.144
0.85	4.8	2	0.566	0.434	0.789		0.154
1.11	3.8	2	0.560	0.440	0.784		0.156
1.44	4.4	2	0.530	0.470	0.888		0.178
1.90	5.2	2	0.502	0.498	0.990		0.198
2.45	6.2	1	0.482	0.518	1.075		0.215
2.78	6.8	1	0.477	0.523	1.096		0.219
3.22	7.6	1	0.448	0.552	1.232		0.256*
3.44	8.0	2	0.400	0.600	1.500		0.300*

[a] P_1 = pressure of MeOH/D mixture. P_2 = pressure of MeONO/MeOCHO mixture. [b] Total pressure in torr. [c] Number of experimental points used in determining K_6 at each P_1/P_2 ratio. [d] All intensities are corrected for mass effects and scaled to 1 for the total ion intensity. [e] Measure of MeOH/MeOD ratio. [f] Values with an asterisk are used in the determination of K_6.

Table II. Summary of Experimental Results Used in Determining K_6

P_1/P_2[a]	10^5P_{TOT}[b]	no. of exptl. points[c]	I_{63}[d]	I_{64}	I_{64}/I_{63}	MeOH/MeOD[e]	K_6
4.0	5.0	6	0.438	0.563	1.284	0.221	0.284
4.5	6.4	8	0.542	0.458	0.845	0.431	0.364
4.6	5.6	3	0.715	0.285	0.399	0.695	0.277
3.0	9.6	5	0.679	0.321	0.473	0.695	0.329
3.8	5.3	3	0.672	0.328	0.488	0.715	0.349
2.2	5.0	3	0.786	0.214	0.272	1.11	0.302
5.6	5.9	1	0.453	0.547	1.208	0.234	0.283

[a] P_1 = pressure of MeOH/D mixture. P_2 = pressure of MeONO/MeOCHO mixture. [b] Total pressure in torr. [c] Number of experimental points used in determining K_6 at each P_1/P_2 ratio. [d] All intensities are corrected for mass effects and scaled to 1 for the total ion intensity. [e] Measure of MeOH/MeOD ratio.

trometer with a rectangular cell.[17,18] Because of space charge effects due to trapped electrons, tuning was difficult and many experiments were performed to obtain reproducibility. All ion populations were obtained by correcting the peak intensities by $1/m$.

The ICR cell was nominally at room temperature while the inlet line chamber was heated to 50 °C in order to improve the control of the pressures of the formates and alchols in the system by reducing the possible condensation within the leak valve orifice. Total pressures were in the range of 2.5×10^{-5} to 1×10^{-4} torr.[19] Both ethyl and methyl nitrite were synthesized by standard procedures.[20] All other compounds were obtained from commercial sources and checked for impurities after several freeze–pump–thaw cycles.

The ab initio calculations were done with the program HONDO[21] on an IBM 3081 computer. Calculations were done with 3-21G,[22] 4-31G,[23] and double-ζ plus polarization basis sets[24] (DZ+P). Geometries were determined with gradient techniques.[25] Force fields were calculated with the 3-21G and 4-31G basis sets at the optimum geometry determined with that basis set. The force fields were determined by numerical differentiation of the gradient.

Method and Results

The reaction scheme used to form the proton-bound dimers of the methoxide anion is shown in Scheme I (reactions 4–6). The methoxide anion is formed by dissociative electron impact of methyl nitrite, with an electron energy of approximately 30 ev.[26,27] Riveros et al.[28] have shown that alkoxides react with alkyl formates to displace CO and form proton-bound alkoxide dimers. In Scheme I, reaction with methyl formate yields the proton-bound methoxide dimer, reaction 5. From the previous experiments carried out by Ellenberger et al. for $[EtOLOEt]^-$,[9] where L = H, D, a pressure ratio of approximately 8:1 for P(EtOCHO):P(EtONO) was shown to give optimum production of the dimer. We employed a similar pressure ratio for P(MeOCHO):P(MeONO) in all of the experiments. The addition of a mixture of methanol and methanol-d_1 leads to ligand exchange with the dimer and equilibrium occurs between the proton- and deuteron-bound dimers. Double resonance experiments have shown that transfers occur in both directions and thus equilibrium can be reached. The data in Figure 1 and Table I demonstrate that equilibrium for reaction 6 is attained. The pressure ratios of methanol/methanol-d_1 and methyl nitrite/methyl formate are held constant, while the relative pressures of [MeOH + MeOD] and [MeOCHO + MeONO] were changed. As shown in Figure 1, as the pressure of the methanol mixture is increased relative to the [MeONO + MeOCHO] pressure, the ratio of $[MeOHOMe]^-$ (m/e 63) to $[MeODoMe]^-$ (m/e 64) rapidly decreases until a constant value is obtained at high pressure. The value of K_6 from

(17) M. R. Ellenberger, R. A. Eades, M. W. Thomsen, W. E. Farneth, and D. A. Dixon, *J. Am. Chem. Soc.*, **101**, 715 (1979).
(18) D. A. Weil, Ph.D. Thesis, University of Minnesota, 1984.
(19) Pressures were measured with an ion gauge and have not been corrected for differential ionization cross sections of the neutrals. Calculation of K_6 does not require knowledge of the absolute pressure of any component.
(20) D. R. Hastie, C. G. Freemann, M. J. McEwan, and H. I. Schiff, *Int. J. Chem. Kinet.*, **8**, 307 (1976).
(21) (a) M. Dupuis, J. Rys, and H. F. King, *J. Chem. Phys.*, **65**, 111 (1976). (b) H. F. King, M. Dupuis, and J. Rys, National Resource for Computer Chemistry Software Catalog, Vol. 1, Program QHO2 (HONDO), 1980.
(22) J. S. Binkley, J. A. Pople, and W. J. Hehre, *J. Am. Chem. Soc.*, **102**, 939 (1980).
(23) R. Ditchfield, W. J. Hehre, and J. A. Pople, *J. Chem. Phys.*, **54**, 724 (1971).
(24) T. H. Dunning, Jr., and P. J. Hay In "Methods of Electronic Structure Theory", H. F. Schaefer, III, Ed., Plenum Press, New York, 1977, p 1.
(25) P. Pulay In "Applications of Electronic Structure Theory", H. F. Schaefer, III, Ed., Plenum Press, New York, 1977, p 153.
(26) R. Farid and T. B. McMahon, *Int. J. Mass Spectrom. Ion Phys.*, **27**, 163 (1978).
(27) (a) D. P. Ridge and J. L. Beauchamp, *J. Am. Chem. Soc.*, **96**, 3595 (1974). (b) S. A. Sullivan and J. L. Beauchamp, *J. Am. Chem. Soc.*, **98**, 1160 (1976).
(28) L. K. Blair, P. C. Isolani, and J. M. Riveros, *J. Am. Chem. Soc.*, **95**, 1057 (1973).

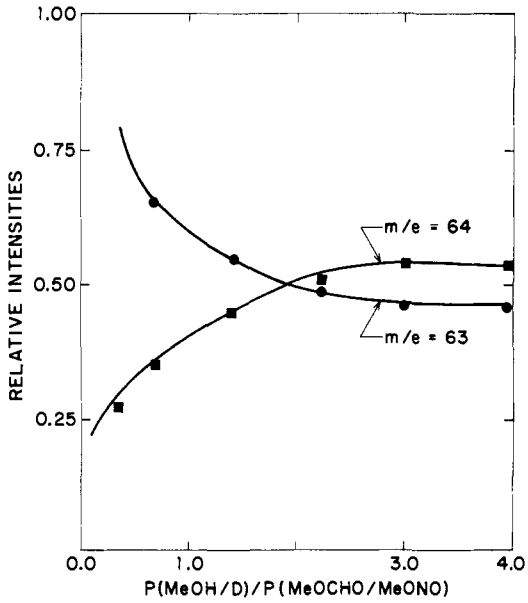

Figure 1. Plot of relative intensity of I_{63} and I_{64} as a function of the ratio of the pressure of the MeOH/D mixture to the pressure of the MeOCHO/MeONO mixture. The figure shows the approach to equilibrium from Scheme I.

Table I is an average of the four starred sets of data giving $K_6 = 0.27$. The [MeOH]/[MeOD] ratio given in Table I was essentially constant (~0.20). Table II is a summary of the experimental results in which the [MeOH]/[MeOD] ratio was varied from 1.1 to 0.2 (at various P_1/P_2 and P_{tot} values). All of the measurements of these K_6 values are at or near equilibrium. The best average value from all of our experimental results is $K_6 = 0.31 + 0.06$.[29]

In order to determine the equilibrium constant K_6, the ratio [MeOH]/[MeOD] within the ICR system was needed. Previous work by Ellenberger et al.[17] suggested that large amounts of H/D exchange probably takes place in the ICR inlet system, in which case the isotope ratio within the cell is different from that in the sample bulb and must be determined in situ.[30] Unlike EtOH/D mixtures, where the isotope ratios could also be measured from the ratio fragmentation peaks at m/e 31 and 32[9] in the positive ion mass spectra, the positive ion mass spectra of the MeOH/D mixtures do not have any such fragmentation peaks.[31] We have shown[18] that the trimethylsilyl cation $SiMe_3^+$, formed by electron impact on tetramethylsilane, readily forms collision complexes with methanol (reaction 7). The ratio of the adduct peaks I_{105}/I_{106}

$$Me_3Si^+ + MeOH/D \longrightarrow Me_3Si^+{-}O(Me)(H(D)) \quad (7)$$

(m/e 105 (106))

(corrected by $1/m$) was used to measure the in situ MeOH/D ratio listed in Tables I and II.[32]

Three different routes were tried in order to determine the isotope fractionation factor for the proton-bound methoxide–ethoxide mixed dimer; none of these were successful. Substitution of EtOH/D for MeOH/D in reaction 6 of Scheme I leads to the dominant formation of the proton-bound dimer of EtO^-. In a second attempt, reaction of MeO^- with EtOCHO is observed to form the mixed proton-bound dimer anion. However, side reactions lead to the formation of the proton-bound dimer of EtO^-, and equilibrium for the mixed species cannot be observed. Finally, the mixed dimer can be formed by dissociative electron bombardment of ethyl nitrite to form the ethoxide anions which then react with methyl formate, yielding the mixed dimer and CO as shown in Scheme II. Although double resonance is observed in both directions for reaction 9, equilibrium was probably not reached since reactions 10a, 10b, and 11 become dominant at high pressures, leading to the formation of proton-bound methoxide dimers.

Scheme II

$$EtO^- + MeOCHO \longrightarrow [MeOHOEt]^- + CO \quad (8)$$
$$[MeOHOEt]^- + MeOD \longrightarrow [MeODOEt]^- + MeOH \quad (9)$$
$$[MeOHOEt]^- + MeOD \longrightarrow [MeOHOMe]^- + EtOD \quad (10a)$$
$$\longrightarrow [MeODOMe]^- + EtOH \quad (10b)$$
$$[MeODOEt]^- + MeOD \longrightarrow [MeODOMe]^- + EtOD \quad (11)$$

Table III. Geometry of $[CH_3O{-}H{-}OCH_3]^-$[a]

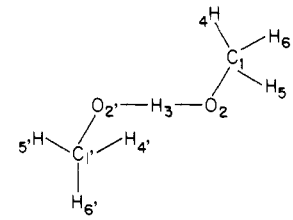

parameter	3-21G	4-31G	DZ+P
$r(C_1{-}O_2)$	1.398	1.384	1.352
$r(C_1{-}H_4)$	1.102	1.103	1.111
$r(C_1{-}H_5)$	1.100	1.104	1.112
$r(C_1{-}H_6)$	1.105	1.104	1.113
$r(C_{1'}{-}O_{2'})$	1.401	1.402	1.375
$r(C_{1'}{-}H_{4'})$	1.100	1.090	1.100
$r(C_{1'}{-}H_{5'})$	1.098	1.088	1.096
$r(C_{1'}{-}H_{6'})$	1.099	1.091	1.099
$r(O_2{-}H_3)$	1.245	1.428	1.417
$r(O_2{-}H_3)$	1.171	1.051	1.035
$r(O_2{-}O_{2'})$	2.414	2.473	2.451
$\theta(O_2C_1H_4)$	112.7	113.1	113.4
$\theta(C_2C_1H_5)$	113.9	113.9	114.2
$\theta(O_2C_1H_6)$	114.6	114.0	114.4
$\theta(H_4C_1H_5)$	105.3	105.1	104.7
$\theta(H_4C_1H_6)$	104.7	104.9	104.8
$\theta(H_5C_1H_6)$	104.6	104.9	104.2
$\theta(C_1O_2H_3)$	108.8	114.1	109.1
$\theta(O_{2'}C_{1'}H_{4'})$	114.6	112.8	113.6
$\theta(O_{2'}C_{1'}H_{5'})$	110.8	109.4	109.6
$\theta(O_{2'}C_{1'}H_{6'})$	114.5	112.7	113.3
$\theta(H_{4'}C_{1'}H_{5'})$	105.5	107.4	106.8
$\theta(H_{4'}C_{1'}H_{6'})$	105.1	106.9	106.3
$\theta(H_{5'}C_{1'}H_{6'})$	105.5	107.4	106.9
$\theta(C_{1'}O_2H_3)$	109.6	110.3	109.9
$\theta(O_2H_3O_{2'})$	174.9	172.5	177.4
$\psi(H_6{-}C_1{-}O_2{-}H_3)$	96.5	94.2	98.1
$\psi(H_{5'}{-}C_1{-}O_2{-}H_3)$	174.0	179.4	176.6
$\psi(C_{1'}{-}O_1{-}O_1{-}C_1)$	106.9	103.6	104.5
energy (au)	−228.190246	−229.142674	−229.540404

[a] All distances in Å. All angles in deg. ψ is a torsion angle.

Computational Results

A set of calculations has been made in order to determine the structure of the proton-bound dimer of the methoxide anion. The initial calculations were done with the 3-21G basis set. At first the geometry was optimized in C_{2h} symmetry in the all-trans structure.

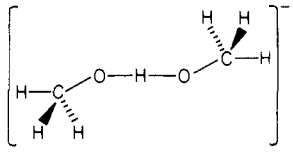

(29) The average value of K_6 was determined by using the value from Table I (an average value of 4 experiments) and the seven values from Table II.

(30) M. R. Ellenberger, M. L. Hendewerk, D. A. Weil, W. E. Farneth, and D. A. Dixon, *Anal. Chem.*, **54**, 1309 (1982).

(31) The parent ions for MeOH and MeOD cannot be used due to the presence of $MeOH_2^+$ and the participation of the parent ions in ion–molecule reactions.

(32) The amount of MeOH and MeOD in the system becomes equal to the peak intensities of the 105 and 106 complexes present corrected by $1/m$. The values are an average of many experiments carried out before and after the negative ion experiments.

Figure 2. Computer graphic structure for [MeOHOMe]$^-$. The plot is generated with the program ANIMOL. The radii for C and O are taken as 1.5× covalent radii and the radius for H is 2.0× covalent radius.

The calculations demonstrated that the symmetric structure is indeed a minimum at this level of basis set given the position of the methyl groups. However, a determination of the force field showed the presence of three negative eigenvalues corresponding to three imaginary frequencies. Subsequent calculations demonstrated that these were due to the torsional motion about the O–O axis and the methyl torsions. The geometry was then optimized in C_1 symmetry with the parameters given in Table III. this was the starting structure for further optimizations. As can be seen in Table III, the structure is asymmetric with respect to the proton interaction with the two oxygens, $r(O_2–H_3)$ and $r(O_2'–H_3)$, but only slightly so. Subsequent optimizations with the 4-31G and DZ+P basis sets lead to structures which are clearly asymmetric as shown in Table III. A computer graphics depiction[33] of the structure is given in Figure 2. Here, the structure can best be described as the interaction of methanol with a methoxide anion. In order to compare the structure of the dimer with the monomers, the geometries for CH_3OH (C_s) and CH_3O^- (C_{3v}) were determined with the DZ+P basis set and are given in Table IV. The methanol-like fragment in the dimer has a longer C–O bond (1.375 Å) than does the methoxide-like fragment (1.352 Å). However, the C–O bond in the methanol-like fragment is substantially shorter than that in methanol. Other differences are the longer C–H bonds and smaller HCH angles in the fragment as compared to methanol and, of course, the quite long O–H bond in the fragment. Thus, the proton is partially transferred to the methoxide. As a consequence, some amount of CH_3O^- character is found in the methanol fragment leading to the above deviations. In the methoxide fragment, the presence of the methanol fragment is large enough to perturb the structure as compared to that of an isolated methoxide ion. The C–O bond is longer in the fragment while the CH bonds are shorter; the HCH angles have also increased in the fragment. The O–H–O bond is approximately linear as would be expected from the structure for [HO–H–OH]$^-$.[11,13,14] The O–O distance is similar to that found in $OH^-\cdots H_2O$ at the 6-31G* level.[11,14b] The orientation of the methyl groups relative to the O–O axis is similar to that found in peroxides. This differs from the structure of the proton-bound dimer of two hydroxides[11,13,14] which has a planar structure.

In order to estimate the barrier to proton transfer from one CH_3O^- to the other, a partially symmetrized structure was constructed. The O–H and C–O bond distances were made equal with the remaining parameters taken from the DZ+P basis set geometry. The DZ+P energy was calculated at this point and gives a barrier of 2.18 kcal/mol (761 cm^{-1}). Since an optimum geometry for the symmetric species was not obtained, this represents an upper limit to the energy of this process.

Table IV. Molecular Geometries of CH_3OH and CH_3O^- [a]

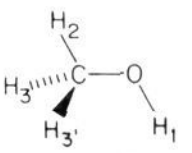

parameter	3-21G	4-31G	DZ+P	exptl[6]
		CH_3OH		
r(C–O)	1.440	1.429	1.403	1.427
r(O–H_1)	0.966	0.951	0.945	0.956
r(C–H_2)	1.079	1.076	1.081	1.096
r(C–H_3)	1.085	1.082	1.088	1.096
θ(C–O–H_1)	110.3	112.9	109.6	108.9
θ(O–C–H_2)	106.4	106.6	107.0	109.9
θ(O–C–H_3)	112.2	111.5	111.9	109.9
θ(H_2–C–H_3)	108.5	109.0	108.5	109.0
θ(H_3–C–H_3')	108.9	109.2	108.9	
energy (au)	−114.398018	−114.871510	−115.074381	
		H_3CO^-		
r(C–O)	1.348	1.362	1.325	
r(C–H)	1.134	1.123	1.128	
θ(O–C–H)	117.3	115.6	115.9	
θ(H–C–H)	100.7	102.6	102.3	
energy (au)	−113.724797	−114.218405	−114.424706	

[a] All distances in Å. All angles in deg. [b] Kojima, T.; Breig, E. L.; Lin, C. C. *J. Chem. Phys.* **1961**, *35*, 2139.

The structure of [MeO–H–OMe]$^-$ has been determined by Jorgenson and Abraham[11] at the SCF level using a 4-31G basis set. A linear OHO bond and a C_s structure were assumed and not all parameters were optimized. The O–O distance of 2.54 Å is longer than our value and the short O–H distance, 1.02 Å, is in good agreement with our larger calculations. No barrier to hydrogen transfer was calculated. The structure of [HO–H–OH]$^-$ has been determined with a large [5s4p1d/3s1p] basis set.[13] The value for the O–O distance is 2.55 Å, and the value for the OH distance is 1.02 Å. The barrier to proton transfer is 1.4 kcal/mol at this level. When correlation effects are included,[13] the OH bond lengthens to 1.09 Å, the O–O distance decreases to 2.47 Å, and the barrier to proton transfer decreases to a value of 0.15 kcal/mol. We would thus expect our calculated barrier to also decrease if correlation corrections and diffuse basis functions were included.

The vibrational frequencies for [MeOHOMe]$^-$ and [MeODOMe]$^-$ determined with the 4-31G basis set are given in Table V. Our discussion focuses on the proton-bound dimer. There are six low-lying modes (<500 cm^{-1}) predicted for the proton-bound dimer as compared to one low-lying mode (the torsion) for the methanol monomer. These low-energy modes are due in part to the methyl torsions, the torsion about the O–O axis, and the stretch of the two O atoms. This latter mode is expected to be at 357 cm^{-1}. The motion of the central proton comes at much higher frequencies. The asymmetric stretch is predicted to occur at 2124 cm^{-1} while the out-of-plane bend similar to the C–O–H bend in the monomer is at 1737 cm^{-1}. The calculated frequencies for CH_3OH, CH_3OD, and CH_3OD^- are given in Table VI. The corresponding OH stretching mode in CH_3OH is much higher, 3975 cm^{-1} (3681 cm^{-1}, exptl), while the bend is lower, 1473 cm^{-1} (1345 cm^{-1}, exptl).[34] The in-plane C–O–H bending mode is at 1454 cm^{-1}. These values can be compared with those for FHF^- which is a symmetric dimer. For FHF^-, the calculated frequencies with the 4-31G basis set are 649, 1307, and 1384 cm^{-1} for the symmetric stretch, the asymmetric stretch, and the bend, respectively. The experimental values known for the latter two are 1364 and 1217 cm^{-1}, respectively.[34] Thus, the motion of the proton in the methoxide dimer is more constrained than motion in the symmetric bifluoride dimer.

(33) R. M. Hilmer Proceedings of the National Computer Graphics Association, submitted 1985.

(34) T. Shimanouchi, "Tables of Molecular Vibrational Frequencies", NSRDS-NBS 39, National Bureau of Standards, Washington, D.C., 1972.
(35) B. S. Ault, *J. Phys. Chem.*, **82**, 844 (1978).

Table V. Vibrational Frequencies for $[MeOHOMe]^-$ and $[MeODOMe]^-$ at the 4-31G Level (in cm^{-1})

	freq	$[MeOHOMe]^-$	$[MeODOMe]^-$
ν_1		3167	3166
ν_2		3120	3120
ν_3		3099	3097
ν_4		2971	2968
ν_5		2931	2930
ν_6		2928	2928
ν_7	[a]	2124	1497
ν_8	[b]	1737	1367
ν_9		1684	1685
ν_{10}		1676	1675
ν_{11}		1669	1669
ν_{12}		1666	1666
ν_{13}		1639	1639
ν_{14}		1592	1708[c]
ν_{15}	[d]	1454	1030
ν_{16}		1272	1280
ν_{17}		1267	1272
ν_{18}		1262	1266
ν_{19}		1243	1157
ν_{20}		1145	1135
ν_{21}		1128	1107
ν_{22}	[e]	357	345
ν_{23}		168	166
ν_{24}		129	128
ν_{25}		106	106
ν_{26}		100	100
ν_{27}		53	53

[a] Asymmetric stretch O–H(D)–O. [b] C–O–H(D) bend-out of plane. [c] Mode with some component of O–D–O asymmetric stretch. [d] C–O–H(D) bend-in plane as in CH_3OH. [e] Mode with large component of O–O stretch.

Table VI. Vibrational Frequencies for CH_3OH, CH_3OD, CH_3O^- at the 4-31G Level (in cm^{-1})

freq	CH_3OH (calcd)	CH_3OH (exptl)[a]	CH_3OD (calcd)	CH_3OD (exptl)[a]	CH_3O^- (calcd)
ν_1 [b]	3975	3681	2897	2718	
ν_2	3337	3000	3338	3000	2778
ν_3	3230	2960	3230	2960	2654
ν_4	3176	2844	3176	2843	2654
ν_5	1679	1477	1679	1473	1669
ν_6	1671	1477	1671	1473	1650
ν_7	1635	1455	1635	1456	1650
ν_8 [c]	1473	1345	928	864	
ν_9	1270	1165	1352	1230	1274
ν_{10}	1158	1060	1270	1160	1274
ν_{11}	1097	1033	1100	1040	1113
ν_{12} [d]	339	295	271	213	

[a] Reference 34. [b] O–H(D) stretch. [c] C–O–H(D) bend. [d] CH_3 torsion.

It is unlikely that our harmonic potential approximation is properly describing the asymmetric motion of the proton. Comparison of the predicted frequency with that of the barrier height to proton transfer shows that the proton, even for the zero-point level, would be above the barrier and thus the harmonic approximation would not hold. A more appropriate potential for describing the motion of the proton would be a double minimum potential. Kreevoy[7] has previously published such a description and we refer to his potential V_3 which has the form $V_3 = 453y^4 - 37.8y^2$ where the energies are in units of 10^3 cm^{-1} and y is in angstroms. The barrier height for this potential is 790 cm^{-1}, and the width of the potential defined as the distance between the two minima is 0.41 Å. This can be compared with our values of 760 cm^{-1} for the barrier height and a distance of 0.38 Å. Solution of the one-dimensional Schrodinger equation for this potential gives a zero-point energy frequency of 690 cm^{-1} for protonic motion and 560 cm^{-1} for motion of a deuteron.

The energy of the hydrogen bond at the DZ+P level is ΔE = 25.9 kcal/mol. The value calculated by Jorgenson and Ibrahim[11] of 25.7 kcal/mol with a smaller basis set and a partially optimized geometry is in good agreement with our value. Inclusion of zero-point effects lowers this value by 0.3 kcal/mol to ΔE_0 = 25.6 kcal/mol. Comparison with experiment requires the value of ΔH for reaction 12 This requires conversion of ΔE_0 (the bond strength

$$MeOH + MeO^- \rightarrow MeOH\cdots OMe^- \qquad (12)$$

at 0 K) to ΔE_{298} and conversion of this value to ΔH_{29}. The translational and rotational degrees of freedom can be treated classically and contribute $-3RT$ to ΔE. In general, vibrational corrections are small; however, the dimer has a number of very low frequency modes and these cannot be neglected. The vibrational correction will lead to a decrease in $\Delta E_{vib}(T)$ of ~3.0 kcal/mol. The conversion term for going from ΔE to ΔH is $-\Delta nRT = -RT$. This gives $\Delta E_0 \sim H_{298} = -25.6$ kcal/mol. The best experimental value for this quantity is -22.3 kcal/mol,[36] and the theoretical value is too high by 3 kcal/mol. This difference is due to a combination of basis set deficiency and correlation corrections. On the basis of results for $[HO-H-OH]^-$, inclusion of diffuse functions would decrease ΔE_0 since CH_3O^- would be treated better relative to the other two structures. (This effect will be smaller in our study than in $[HO-H-OH]^-$ since we have more basis functions due to the presence of the methyl group.) Correlation corrections would be expected to increase ΔE_0 and thus the two computational effects partially cancel.

Discussion

The value of the gas-phase isotope fractionation factor of the proton-bound methoxide dimer is defined by K_{13}. Water is the usual standard-state adopted by solution-phase experimentalists because it commonly equilibrates with the types of compounds that are typically studied.[37,38] To obtain the gas-phase isotope

$$[MeOHOMe]^-_{(g)} + HOD_{(l)} \rightleftharpoons [MeODOMe]^-_{(g)} + H_2O_{(l)} \qquad (13)$$

fractionation factor for the proton-bound methoxide dimer from K_6, the value of ϕ for methanol in the gas phase must be calculated. This value can be obtained from the equilibrium constants K_{14} and K_{15}. The value for K_{14} is 1.12 ± 0.04.[39] The value for K_{15}

$$MeOH_{(l)} + HOD_{(l)} \rightleftharpoons MeOD_{(l)} + H_2O_{(l)} \qquad (14)$$

$$MeOH_{(g)} + MeOD_{(l)} \rightleftharpoons MeOD_{(g)} + MeOH_{(l)} \qquad (15)$$

is simply the ratio of vapor pressures (V_p) and $K_{15} = V_p(MeOD)/V_p(MeOH) = 0.95$.[39,40] Multiplication of K_6 by the above correction factors gives a value for $\phi_{gp} = 0.33 \pm 0.06$ related to the standard state and $\phi_{gp} \cong K_6$.

In pure methanol, $\phi(MeOLOMe)^- = 0.74$ as determined from NMR measurements.[10] To investigate the effect of solvation on the isotope fractionation factor, Baltzer[10a] decreased the concentration of methanol from that in the pure solution by adding dimethyl sulfoxide (Me_2SO) and found that ϕ decreases from 0.74 to 0.38 as the concentration of [MeOH] decreases from 100% to 25% MeOH. Our gas-phase results are comparable to the solution-phase value when X_{Me_2SO} is extrapolated to 100%, giving $\phi = 0.3$. This suggests that the methoxide anion is only singly solvated at low concentration in Me_2SO was postulated by Baltzer.[10a]

The equilibrium constant for reaction 6 can in principle be calculated from partition functions. However, this requires all of the normal mode frequencies and, as discussed above, we cannot directly determine all of the frequencies from the region of the surface that we have calculated. To a first approximation, the value for K_6 is given by the following expression

$$K_6 = \exp\left[\frac{hc}{kT}(\Delta ZPE_{complex} - \Delta ZPE_{monomer})\right] \qquad (16)$$

(36) G. Caldwell and P. Kebarle, private communication.
(37) (a) V. Gold, *Trans. Faraday Soc.*, **56**, 225 (1960). (b) A. J. Kresge, *Pure Appl. Chem.*, **8**, 243 (1964). (c) W. J. Alberty In "Proton Transfer Reactions", E. F. Caldin and V. Gold, Eds., Chapman and Hall, 1975, p 263.
(38) G. Sicking, *Ber. Bunsen.-Ges. Phys. Chem.*, **76**, 790 (1972).
(39) D. E. Clegg and J. H. Rolston, *J. Chem. Soc., Chem. Commun.*, 1037 (1978).
(40) G. Jancso and W. A. Van Hook, *Chem. Rev.* **74**, 689 (1974).

where ΔZPE is the difference in zero-point energies between AHA^- (AH) and ADA^- (AD). The value for ΔZPE was determined as one-half the sum of the vibrational frequencies for each species except as described below. For CH_3OH and CH_3OD, the calculated value for ΔZPE is 746 cm^{-1} as compared to an experimental value of 681 cm^{-1}.[34] (This latter value is not precise as the torsional frequency is not well-determined experimentally.) For the proton-bound dimers the situation is complicated by the fact that the asymmetric stretch of the proton (deuteron) is not well-treated in the harmonic approximation. We thus define the ZPE to be one-half the sum of all of the modes excluding the asymmetric stretch. We take the value for the asymmetric stretch zero-point frequency from that determined for the model potential V_3. The value for ΔZPE for the asymmetric stretch is 130 cm^{-1}. (Examination of Kreevoy's other potentials[7] shows that ΔZPE is not strongly dependent on the barrier height and even with no barrier has a value of 200 cm^{-1}.) The asymmetric stretch in the proton-bound dimer is quite distinct. Although this mode can be found in the deuteron-bound dimer, there is also a slightly higher lying mode with some asymmetric stretch character. From the above results, the calculated ΔZPE for the dimer is 530 cm^{-1}. Substitution into eq 16 gives a calculated value for K_6 of 0.35, in excellent agreement with the observed value of 0.31, especially considering the approximations made in determining ΔZPE and in the use of eq 16. The use of eq 16 assumes that the ratio of the translational, rotational, and electronic partition functions is unity. This should be a good approximation since there should not be large isotope effects on these quantities. Another approximation in eq 16 is that the temperature dependences of the vibrational populations were neglected. Examination of the vibrations for the dimers shows that this is not that severe an approximation for $AH(D)A^-$ since the lowest lying modes (those that would be thermally populated) do not exhibit a large isotope dependence. This is not surprising since the vibrational modes involving the proton (deuteron) are at higher frequencies. There is likely to be a larger contribution from the monomer since the torsional potential does exhibit some isotope effect.

The good agreement of the calculated value of K_6 with the experimental value is consistent with Kreevoy's discussion[7] of the role of the bending modes in raising the value of ϕ from that predicted by using only the asymmetric stretch. Although his discussion was qualitative, our results demonstrate that the modes external to the asymmetric stretch will indeed raise the value ϕ and thus moderate the isotope effect. However, the value for ϕ_{gp} is still far from unity and demonstrates the presence of a large isotope effect. Comparison with our previous work on $A = EtO^-$ shows that substitution of Et for Me raises ϕ_{gp} from 0.33 to 0.46. Whether this is due to a change in the central barrier height or to the presence of additional modes external to the asymmetric stretch cannot be determined at this time.

Registry No. Methoxide anion, 3315-60-4.

Reversible Formation and Disruption of Micelles by Control of the Redox State of the Head Group

T. Saji,* K. Hoshino, and S. Aoyagui

Contribution from the Department of Chemical Engineering, Tokyo Institute of Technology, Ohokayama, Meguro-ku, Tokyo 152, Japan. *Received January 3, 1985*

Abstract: Electrochemical and spectroscopic studies of a functional surfactant, (ferrocenylmethyl)dodecyldimethylammonium bromide (I^+) with ferrocene as the redox moiety, are reported. The concentration dependence of the diffusion coefficient values for I^+ and its oxidized form I^{2+} show that the I^+ surfactants form redox-active micelles and that these micelles can be broken up into monomers by oxidation and re-formed by reduction. Feasibility of such reversible control of the formation–disruption of micelles is also demonstrated by a spectroscopic observation that a dye is solubilized or released according as the micelles are formed or broken up. In addition, the result of potential-step chronoamperometry is interpreted on the basis of the Nernst diffusion-layer model.

Functional micelles, i.e., aggregates of surfactant molecules to which functional groups are covalently bonded, possess advantages over nonfunctional ones in the following aspects: (1) ability to undergo specific reactions, e.g., redox reactions,[1,7] (2) effective charge separation by using the functional surfactant as an electron acceptor,[2-4] (3) reaction media in concentrating or fixing active sites,[5] and (4) probes for the microenvironment of micelles.[6] No studies have so far dealt with the effect of functional groups on the dynamic properties of micelles, e.g., the self-assembling behavior, or the static ones, e.g., the CMC and the aggregation number. The present paper deals with the reversible formation and disruption of micelles by control of the redox state of the surfactant-head group.[7] The electroactive surfactant studied is the bromide salt of $FcCH_2N^+(CH_3)_2C_{12}H_{25}$ (I^+), where Fc represents the ferrocene moiety.

Experimental Section

The bromide salt of I^+ was prepared by the following procedures: The mixture of equimolar amounts of ((dimethylamino)methyl)ferrocene (Aldrich) and *n*-dodecyl bromide (Tokyo Kasei) was stirred for 2 h at 60 °C. The reaction product was recrystallized twice from acetone to give a yellow, crystalline product in 63% yield. It was identified by the elemental analysis. Calcd for $C_{25}H_{42}NFeBr$: C, 60.9; H, 8.6; N, 2.7. Found: C, 60.8; H, 8.6; N, 2.7. The IR and the electronic spectra for I^+ were respectively in fair agreement with those for ferrocene.[8] Li_2SO_4

(1) Takuma, K.; Sakamoto, T.; Nagamura, T.; Matsuo, T. *J. Phys. Chem.* **1981**, *85*, 619.
(2) Brugger, P. A.; Grätzel, M. *J. Am. Chem. Soc.* **1980**, *102*, 2461.
(3) Brugger, P. A.; Infelta, P. P.; Braun, A. M.; Grätzel, M. *J. Am. Chem. Soc.* **1981**, *103*, 320.
(4) Humphry-Barker, R.; Grätzel, M.; Tundo, P.; Plelizetti, E. *Angew. Chem., Int. Ed. Engl.* **1979**, *18*, 630.
(5) Fendler, J. H. "Membrane Mimetic Chemistry"; Wiley: New York, 1982; pp 339-409.
(6) Menger, F. M.; Chow, J. F. *J. Am. Chem. Soc.* **1983**, *105*, 5501.
(7) The preliminary study of the reversible formation and disruption of micelles by control of the redox state of the head group was reported: Saji, T.; Hoshino, K.; Aoyagui, S.; *J. Chem. soc., Chem. Commun.* **1985**, 865.

0002-7863/85/1507-6865$01.50/0